# A COMPARISON OF "SPATIALLY AVERAGED EULERIAN" AND "SEMI-LAGRANGIAN" TREATMENTS OF MOUNTAINS

H Ritchie and M Tanguay
Recherche en prévision numérique
Service de l'environnement atmosphérique
Dorval, Québec, Canada H9P 1J3

Abstract: It has been demonstrated previously by both analysis and numerical integration that there is a serious problem incorporating orographic forcing into semi-implicit semi-Lagrangian models, since spurious resonance can develop in mountainous regions for Courant numbers larger than unity. Rivest *et al.* (1994) recommended using a second-order instead of a first-order semi-implicit off-centering to eliminate the spurious resonances, the former being more accurate. The present study shows by a linear one-dimensional analysis that a first-order semi-implicit off-centering can be used more effectively to eliminate the spurious resonances when combined with a *spatially-averaged Eulerian* instead of a *semi-Lagrangian* treatment of mountains. The analysis reveals that the resonance is much less severe with the spatially-averaged Eulerian treatment of mountains, and hence can be suppressed with a weaker first-order off-centering. This combination could represent a valid alternative to second-order off-centering which needs extra time levels. These various points are illustrated with both barotropic and baroclinic semi-implicit semi-Lagrangian models. An important feature of the baroclinic model formulation is the inclusion of topography in the basic state solution that is used for the semi-implicit treatment of the gravity-wave producing terms. In tests run from real data it appears that, in current three-time-level models, simply changing from the semi-Lagrangian to the spatially-averaged Eulerian treatment of mountains is sufficient to significantly reduce the topographic resonance problem, permitting the use of larger timesteps that produce acceptable time truncation errors without provoking the fictitious numerical amplification of short scale waves.

## 1. INTRODUCTION

In semi-implicit models, a semi-Lagrangian treatment of advection improves model efficiency by permitting larger timesteps than those allowed by Eulerian advection schemes. For this reason, since the initial demonstration by Robert *et al.* (1985) in a hydrostatic primitive equations model, this method is being used in an increasing number of weather forecasting and climate centers (e.g., Tanguay *et al.* 1989; McDonald and Haugen 1992; Bates *et al.* 1993; Purser and Leslie 1994; Ritchie and Beaudoin 1994; Williamson and Olson 1994; Ritchie *et al.* 1995). However, it has been demonstrated by both analysis and numerical integration that there is a serious problem incorporating orographic forcing into semi-implicit semi-Lagrangian models, since spurious resonance can develop in mountainous regions for Courant numbers larger than unity (Kaas 1987; Coiffier *et al.* 1987; Tanguay *et al.* 1992; Rivest *et al.* 1994). In practice this inhibits the overall efficiency advantage of the semi-Lagrangian treatment of advection, since at high spatial resolution the fictitious numerical amplification of the resonant stationary short scale waves locally contaminates the flow patterns before the timesteps become large enough for the time truncation errors of the transient waves to become unacceptable.

Some possible solutions for this problem have been proposed. In the context of a two-time-level scheme Rivest *et al.* (1994) clarified the source of the problem and recommended using a second-order off-centering of the semi-implicit averaging along the trajectory. Recently Côté *et al.* (1995) have examined the possibility of evaluating the semi-Lagrangian derivative using an additional time level of information. The advantage of these approaches is that the time truncation errors remain second-order accurate, but the disadvantage is that they imply the expense of evaluating terms at an extra time level in the time integration scheme. A similar comment applies to a four-time-level retrofit that Rivest and Staniforth (1995) examined for conventional three-time-level schemes. Héreil and Laprise (1995) have also tested the Rivest *et al.* (1994) solution in the context of a three-time-level mesoscale model.

In the present study we examine a very convenient alternative for conventional three-time-level models. If the previous studies are recast in terms of geopotential height perturbations rather than the geopotential thickness perturbations which were used, we see that they have used a semi-Lagrangian treatment of the mountains. However, since the mountains are stationary, the influence of topography can be readily represented as an Eulerian or kinematic forcing. By including this forcing among the terms that are treated with the spatial averaging that is used in many current three-time-level models, the severity of the resonance problem can be greatly reduced. To formally eliminate the resonance it is still necessary to introduce some damping mechanism, such as the first-order off-centering introduced by Tanguay *et al.* 1992, but the required amount is correspondingly reduced with the spatially-averaged Eulerian treatment of mountains. In practice with the timesteps currently used in three-time-level models, simply changing from the semi-Lagrangian to the spatially-averaged Eulerian treatment of mountains appears to be sufficient to suppress the contamination of the forecasts by unrealistic short scale details generated by the presence of topography, without reducing the accuracy of the time integration scheme. This approach is an attractive alternative to other treatments requiring extra time levels.

## 2. LINEAR ANALYSIS OF SHALLOW-WATER EQUATIONS

### 2.1 Linearized equations

In order to examine the spurious resonance of semi-Lagrangian schemes in spectral models in a simpler context, the spectral shallow water model presented by Ritchie (1988) (hereinafter referred to as R88) has been modified to include mountains and first-order off-centering. As a consequence, in the continuity equation (29) of R88 the perturbation geopotential $\Phi$ is replaced by

$$\Phi - \Phi_S$$

where $\Phi_S$ is the geopotential height associated with the surface topography. In order to incorporate the first-order off-centering, the semi-implicit time average applied to the gravity-wave producing terms will be discretized as

$$\overline{(\ )}^t = \frac{1+\delta}{2}(\ )^+ + \frac{1-\delta}{2}(\ )^- \tag{1}$$

where $\delta$ is the off-centering parameter.

For simplicity we assume a constant Coriolis parameter f and do a semi-implicit treatment of the Coriolis term. Expressed in terms of the wind images (U,V) as defined in R88, the linearized momentum equation takes the form

$$\frac{d_L}{dt}U - \overline{fV}^t + \overline{\frac{1}{a^2}\frac{\partial}{\partial\lambda}\Phi}^t = 0 \tag{2}$$

$$\frac{d_L}{dt}V + \overline{fU}^t + \overline{\frac{\cos\theta}{a^2}\frac{\partial}{\partial\theta}\Phi}^t = 0 \tag{3}$$

and the continuity equation becomes

$$\frac{d_L}{dt}\left(\Phi - \Phi_s\right) + \Phi^*\overline{D}^t = 0 \tag{4}$$

where the linear Lagrangian derivative operator is

$$\frac{d_L}{dt}(\ ) = \frac{\partial}{\partial t}(\ ) + \omega\frac{\partial}{\partial\lambda}(\ ) \tag{5}$$

and the semi-implicit time average is given by (1). Here $\omega$ is a constant advecting angular velocity used for the linearization. The other symbols have the same meanings as in R88. Form (4) gives what we will call the semi-Lagrangian treatment of the mountains and is equivalent to the formulation examined by Rivest *et al.* (1994) which can be shown by rewriting (2)-(4) in terms of the thickness perturbation $\phi=\Phi-\Phi_s$ . By applying (5) to the topographic term in (4) and using the fact that topography is steady in time, (4) can be rewritten as

$$\frac{d_L}{dt}\Phi + \Phi^*\overline{D}^t = \omega\frac{\partial}{\partial\lambda}\Phi_s \tag{6}$$

which gives what we will refer to as the Eulerian treatment of the mountains.

We look for solutions of the form

$$g = g_n^m\, e^{im(\lambda-\gamma t)}\, P_n^m(\mu) \tag{7}$$

where $g_n^m$ is the spectral coefficient of a wave-like solution with east-west wave number m, having numerical phase speed $\gamma$, and $P_n^m$ represents a normalized Legendre function whose argument is $\mu = \sin\theta$. We will examine analytic and numerical solutions for these linearized equations.

## 2.2 Analytic forced response

For stationary solutions ($\gamma = 0$) we find that the analytic perturbation geopotential height is given by

$$\left(\Phi_A\right)_n^m = -\frac{\left(\frac{m}{n} F_n\right)^2 - \left(\frac{f}{G_n}\right)^2}{1 - \left(\frac{m}{n} F_n\right)^2} \left(\Phi_s\right)_n^m \tag{8}$$

where

$$G_n^2 = \tilde{n}^2 \Phi^* + f^2$$

and $F_n$ is the Froude number defined as

$$F_n \equiv \frac{n\omega}{G_n} . \tag{9}$$

For synoptic scale motions with $\omega$ approximated as U/a where U represents the advecting wind speed, we find that

$$F_n \approx \frac{U}{\sqrt{\Phi^*}}$$

which is the Froude number as used in Rivest *et al.* (1994). Furthermore, (8) can be approximated as

$$\left(\Phi_A\right)_n^m \approx -\left(\frac{m}{n} F_n\right)^2 \left(\Phi_s\right)_n^m . \tag{10}$$

For the actual case that will be examined in section 4, the scales give values of approximately

$$3*10^{-2} \text{ for } \left(\frac{m}{n} F_n\right)^2 \text{ and } 10^{-3} \text{ for } \left(\frac{f}{G_n}\right)^2 . \tag{11}$$

## 2.3 Numerical forced response

For stationary solutions we find that the numerical perturbation geopotential height is given by

$$\left(\Phi_N'\right)_n^m = -\frac{\left(\frac{S}{\xi}\right)^2 \left(\frac{m}{n} F_n\right)^2 - C^2 \left(\frac{f}{G_n}\right)^2}{C^2 - \left(\frac{S}{\xi}\right)^2 \left(\frac{m}{n} F_n\right)^2} \frac{\sin \xi}{S} \left(\Phi_s\right)_n^m \tag{12}$$

for the semi-Lagrangian treatment of mountains, and by

$$\left(\Phi_N\right)_n^m = \frac{\xi}{\tan\xi}\left(\Phi_N'\right)_n^m \tag{13}$$

for the spatially-averaged Eulerian treatment of mountains where

$$i\,\frac{S}{\Delta t} = i\,\frac{\sin m\Delta t(\omega-\gamma)}{\Delta t} + d_n e^{im\Delta t(\omega-\gamma)}$$

$$C = \cos m\Delta t(\omega-\gamma) + i\,\delta \sin m\Delta t(\omega-\gamma) + \left(1+\delta\right) d_n\, \Delta t\, e^{im\Delta t(\omega-\gamma)}\ ,$$

$s = \sin\xi$ , $c = \cos\xi$ , and $\xi = m\omega\Delta t$ and

$$d_n = \nu\left\{\frac{n(n+1)}{a^2}\right\}^p \tag{14}$$

in which $\nu$ is the diffusion coefficient and p controls the degree of a split-implicit diffusion.

As in Rivest *et al.* (1994) we consider response R defined as the ratio of the numerical and analytic solutions. From (12) / (8) we get

$$R' = \frac{\left\{1-\left(\frac{m}{n}F_n\right)^2\right\}\left\{\left(\frac{S}{\xi}\right)^2\left(\frac{m}{n}F_n\right)^2 - C^2\left(\frac{f}{G_n}\right)^2\right\}}{\left\{\left(\frac{m}{n}F_n\right)^2-\left(\frac{f}{G_n}\right)^2\right\}\left\{C^2-\left(\frac{S}{\xi}\right)^2\left(\frac{m}{n}F_n\right)^2\right\}}\ \frac{\sin\xi}{S} \tag{15}$$

for the semi-Lagrangian treatment of mountains, and (13) / (8) gives

$$R = \frac{\xi}{\tan\xi}\ R' \tag{16}$$

for the spatially-averaged Eulerian treatment of mountains.

## 2.4 Resonances

Next we compare the responses near resonance. In the absence of off-centering and damping for stationary waves, (15) can be rewritten as

$$R' = \frac{\left\{1 - \left(\frac{m}{n} F_n\right)^2\right\}\left\{\left(\frac{m}{n} F_n \frac{\tan \xi}{\xi}\right)^2 - \left(\frac{f}{G_n}\right)^2\right\}}{\left\{\left(\frac{m}{n} F_n\right)^2 - \left(\frac{f}{G_n}\right)^2\right\}\left\{1 - \left(\frac{m}{n} F_n\right)^2 \left(\frac{\tan \xi}{\xi}\right)^2\right\}} \tag{17}$$

and we use (16) for R.

Resonance occurs when the denominator vanishes. Thus R' and R both have resonances when

$$\frac{\tan\xi_R}{\xi_R} = \pm \frac{1}{\frac{m}{n} F_n} \tag{18}$$

which is large in absolute value, since the Froude number is small. Hence there are twin resonant values $\xi_R$ close to $\xi_l = (2\,l + 1)\,\pi/2$ for integer values of l.

Let $\xi_R = \xi_l + \Delta_R$ where $\Delta_R$ is small. Taylor series expansions lead to

$$\tan\xi_R = -\frac{1}{\Delta_R} + O(\Delta_R)$$

and (18) gives

$$\Delta_R \left(\xi_l + \Delta_R\right) = \pm \frac{m}{n} F_n + O\left(\Delta_R{}^3\right)$$

whence

$$\xi_R \approx \xi_l \pm \frac{\frac{m}{n} F_n}{\xi_l} . \tag{19}$$

To find the leading order behavior near $\xi_R$ , let $\xi = \xi_R + \varepsilon$ and consider the dominant behavior as $\varepsilon$ tends to zero. Using (18), (19) and Taylor series expansions leads to dominant behavior

$$\frac{\tan\xi}{\xi} \approx \frac{1}{\pm \frac{m}{n} F_n - \varepsilon\, \xi_l} . \tag{20}$$

Combining the scaling (11) with (20) in (17) yields

$$R' \approx \pm \frac{1}{\frac{m}{n} F_n} \frac{1}{2\,\varepsilon\,\xi_I} \tag{21}$$

as $\varepsilon$ tends to zero, which together with (16) produces

$$R \approx -\frac{1}{2\,\varepsilon\,\xi_I} \,. \tag{22}$$

These resonances are both first order singularities in $\varepsilon$. Since the Froude number is small, R as given by (22) is much smaller than R' as given by (21); that is, the resonance is much weaker with the spatially-averaged Eulerian treatment of mountains.

Now we examine the impact of the first-order off-centering near resonance. With $\delta \neq 0$ and $d_n = 0$ we get $S = s$, $C = c + i\delta s$, and together with the scaling (11), at resonance (18) the responses (15) and (16) become

$$R' \approx -\frac{1}{\left(\delta\xi_R\right)^2 \pm i\,2\delta\left(\frac{m}{n} F_n\right)\xi_R} \tag{23}$$

and

$$R \approx \pm \frac{\frac{m}{n} F_n}{\left(\delta\xi_R\right)^2 \pm i\,2\delta\left(\frac{m}{n} F_n\right)\xi_R} \,. \tag{24}$$

Thus the first-order off-centering can effectively suppress the resonance and produce a finite response, but since the Froude number is small, (24) shows that the weaker resonance at $\xi_R$ with the spatially-averaged Eulerian treatment of mountains can be controlled with a weaker first order off-centering than with the semi-Lagrangian treatment of mountains (23).

## 3. ILLUSTRATIONS WITH SHALLOW WATER MODELS

To graphically demonstrate the advantages of the spatially-averaged Eulerian treatment of the mountains, the numerical and analytic linear solutions for the shallow water equations have been reconstituted for the case of constant angular flow across an isolated "Gaussian hill". This topography (in meters) is shown in figure 1 and the analytic stationary geopotential height produced by combining linear waves whose amplitudes are given by (8) is shown in figure 2, where the central values are in decameters and the contour interval is 2 meters. The numerical solution with a semi-Lagrangian treatment of the mountains (12) with $\delta$=0 and $d_n$=0 is shown in figure 3, and the corresponding numerical solution with the spatially-averaged Eulerian treatment

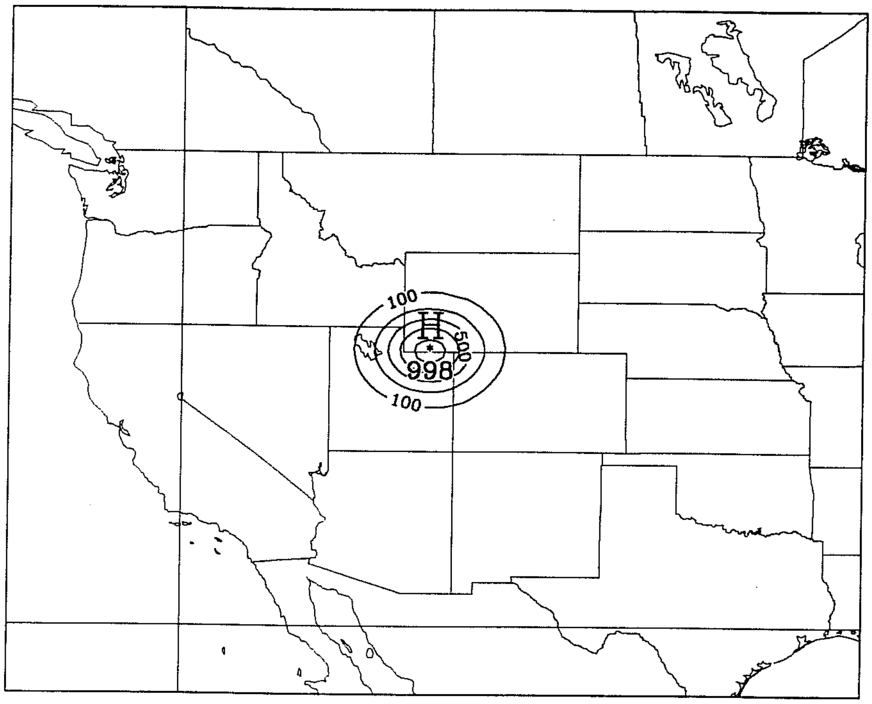


Fig.1 "Gaussian Hill" topography (in meters) for which linear shallow water model stationary responses are reconstituted for constant angular flow.

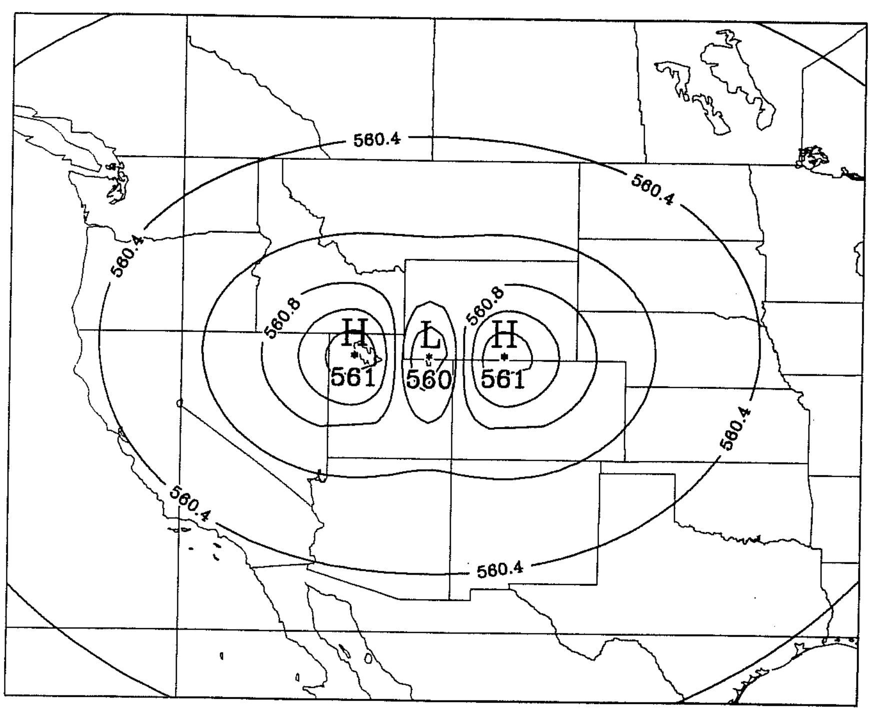


Fig.2 Analytic stationary geopotential height (in decameters) for the case of constant angular flow across the topography depicted in Fig.1. Contour interval 2 meters.

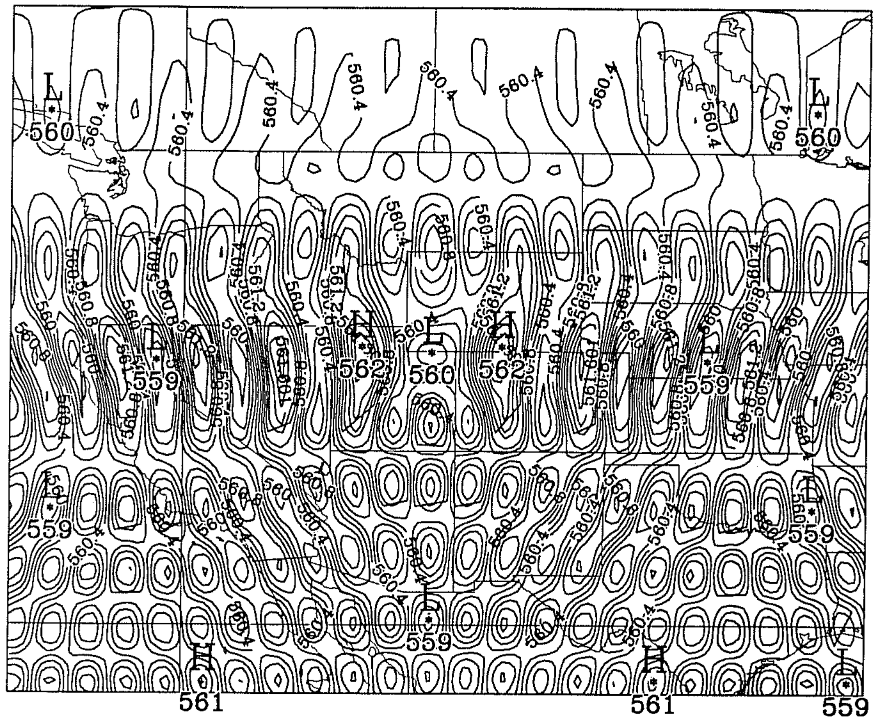


Fig.3 As in Fig.2 except for a numerical solution with a semi-Lagrangian treatment of the mountains. The off-centering parameter is zero.

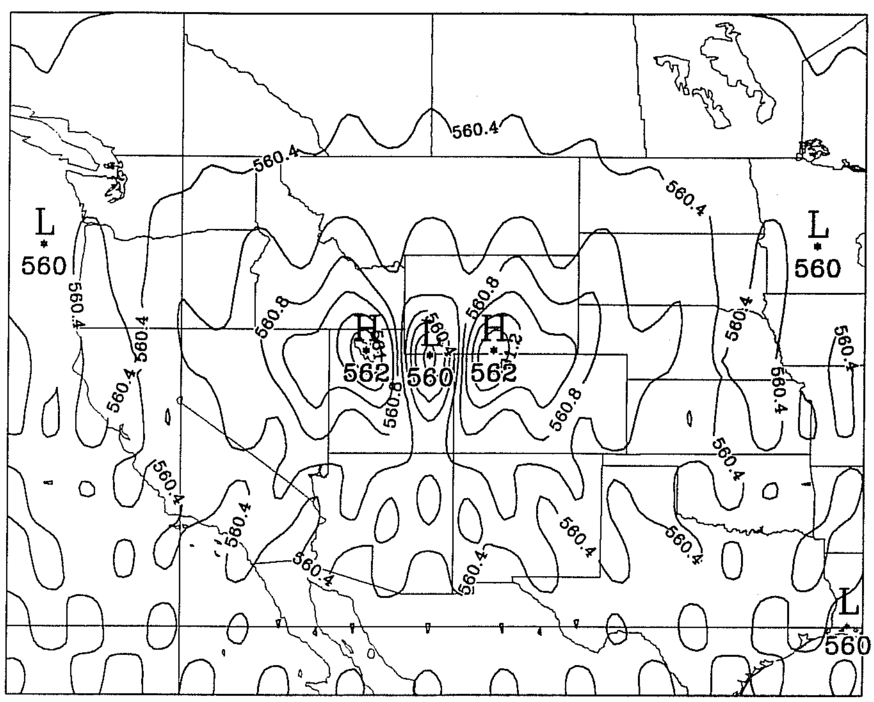


Fig.4 As in Fig.2 except for a spatially-averaged Eulerian treatment of the mountains.

of the mountains (13) is presented in figure 4. The presence of fictitiously amplified short waves is evident in both of figures 3 and 4, but it is clear that these waves are much weaker in figure 4 which bears a much closer resemblance to the analytic solution in figure 2 than figure 3 does. Figures 5 and 6 present the numerical solutions corresponding to figures 3 and 4 respectively except that a weak first-order off-centering of $\delta = .1$ has been added. It is seen that some fictitiously amplified short waves are still evident with the semi-Lagrangian treatment of the mountains (figure 5), whereas the spatially-averaged Eulerian treatment (figure 6) gives a numerical solution that is very close to the analytic one shown in figure 2.

Topography was added to the nonlinear shallow water equations model (R88) and a test was performed with real data for the same case as examined by Rivest *et al.* (1994) starting from an analysis valid at 1200 UTC 12 February 1979. The model was run using a triangular truncation with 120 waves and a timestep of 1800 s. The 48 hour forecast of the 500 mb geopotential height (in decameters), valid at 1200 UTC 14 February 1979, produced by a model with a semi-Lagrangian treatment of the mountains is shown in figure 7, where short waves are evident over Montana and the neighboring states. The corresponding forecast using a model with the spatially-averaged Eulerian treatment of the mountains (without off-centering) is shown in figure 8. It is clear that simply changing the mountain formulation without even introducing off-centering can significantly reduce the manifestation of numerical amplification.

## 4. FORMULATION AND TESTS WITH A BAROCLINIC SPECTRAL MODEL

In this section we examine a spatially-averaged Eulerian treatment of mountains for a baroclinic model. This is achieved by adapting the model presented in Ritchie (1991) and extended by Tanguay *et al.* (1992) and Ritchie and Beaudoin (1994). As a preliminary step, topography is included in the basic state solution that is introduced for the semi-implicit treatment of the gravity-wave producing terms. If we look for a basic state solution at rest, the horizontal momentum equation becomes

$$\nabla\Phi^* + R\,T^*\nabla q^* = 0 \qquad (25)$$

and the hydrostatic equation is

$$\frac{\partial\Phi^*}{\partial\sigma} = -\frac{RT^*}{\sigma} , \qquad (26)$$

where a * superscript denotes the basic state variables, $\Phi$ is the geopotential height, T is the

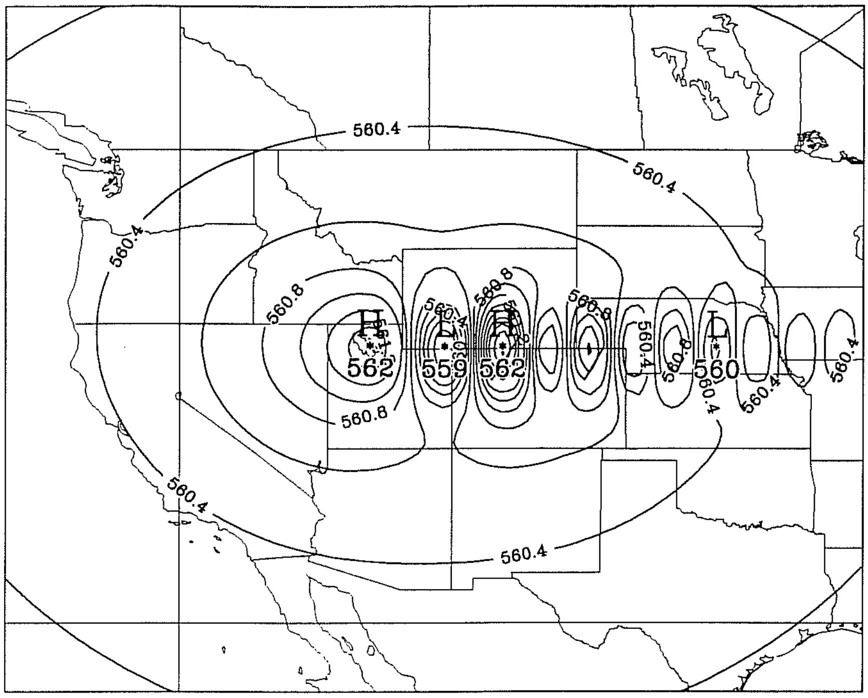


Fig.5 As in Fig.3 except that the first-order off-centering parameter is .1.

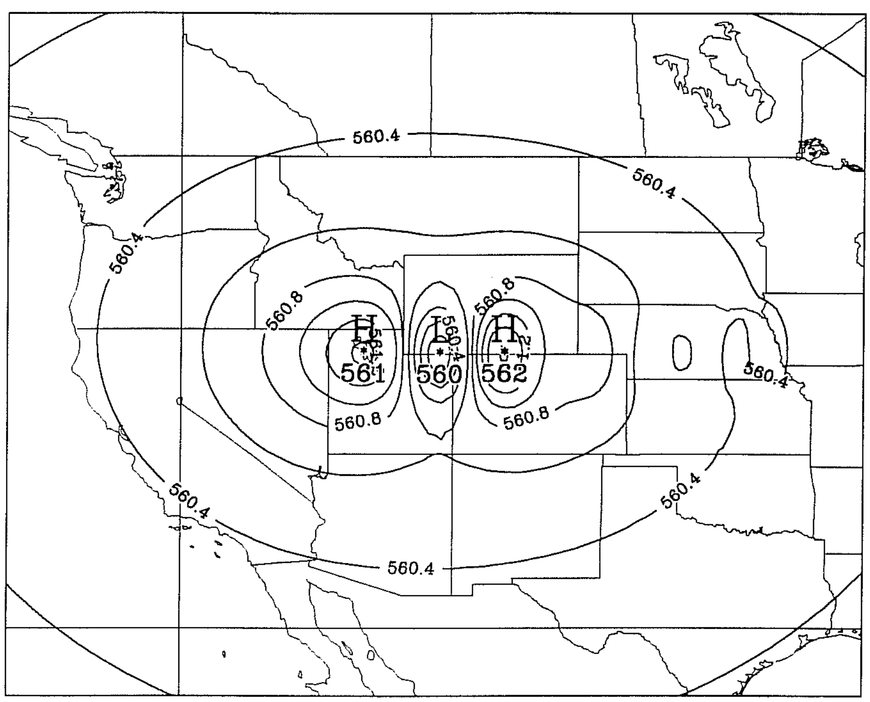


Fig.6 As in Fig.5 except for a spatially-averaged Eulerian treatment of the mountains.

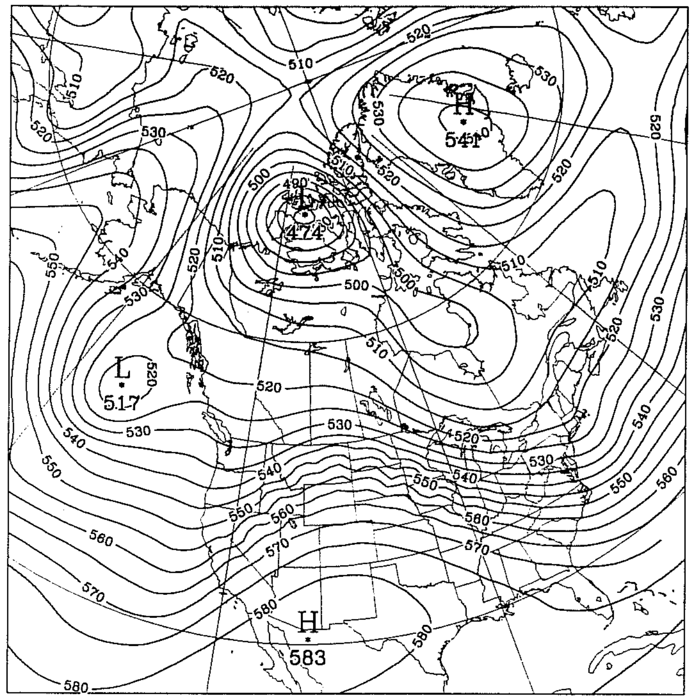

Fig. 7 48 h forecast of the 500 mb geopotential height (dam), valid at 1200 UTC 14 February 1979, produced using a shallow water model with a semi-Lagrangian treatment of the mountains. Contour interval 5 dam.

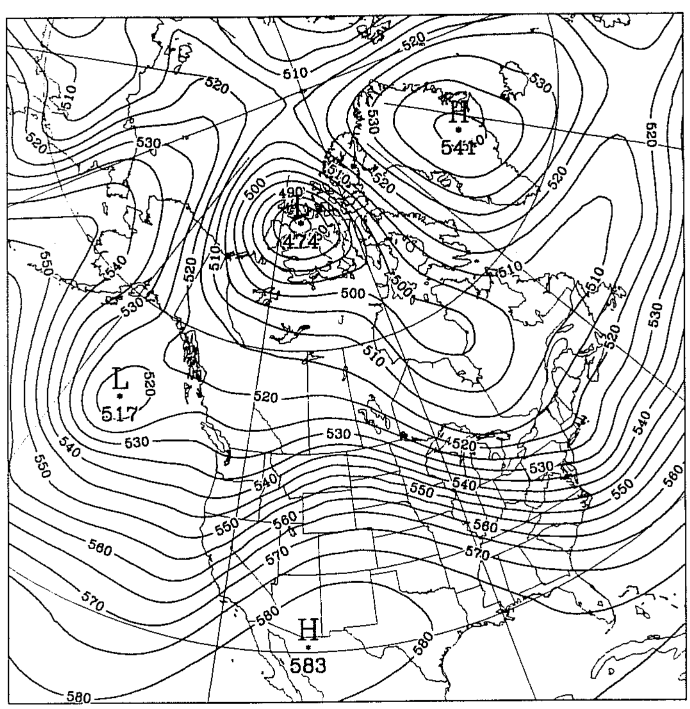

Fig.8 As in Fig.7 except for a spatially-averaged Eulerian treatment of the mountains.

temperature, $q$ = log(surface pressure), R is the gas constant, $\sigma$ is the conventional (pressure)/(surface pressure) vertical coordinate (Phillips, 1957) and $\nabla$ is the horizontal gradient operator with $\sigma$ held constant. Integrating (26) in the vertical gives

$$\Phi^* = \Phi_s + R \int_\sigma^1 \frac{T^*}{\tilde{\sigma}} d\tilde{\sigma} .$$

If $T^* = T^*(\sigma)$ then (25) gives

$$\nabla(\Phi_s + RT^*q^*) = 0$$

from which it follows that

$$q^* = \frac{A(\sigma)}{RT^*(\sigma)} - \frac{\Phi_s}{RT^*(\sigma)}$$

where $A(\sigma)$ is an arbitrary function of $\sigma$. Since $q^*$ is independent of $\sigma$, we conclude that $T^*$ must be a constant unless $\Phi_s = 0$. Consequently for our semi-implicit linearization we use

$$T = T^* + T' \text{ where } T^* = \text{constant}, \tag{27}$$

$$\Phi = \Phi^* + \phi' \text{ where } \Phi^* = \Phi_s - RT^* \ln\sigma, \tag{28}$$

$$\text{and } q = q^* + q' \text{ where } q^* = - \Phi_s / ( RT^*) . \tag{29}$$

We define the generalized perturbation geopotential as

$$P' = \phi' + RT^*q'$$

$$= \Phi + RT^* \ln\sigma + RT^* q . \tag{30}$$

The momentum equation and hydrostatic equation retain exactly the same form that they had in Ritchie (1991). The thermodynamic equation becomes

$$\frac{dT'}{dt} - \gamma\left(\frac{dq'}{dt} + \frac{\dot{\sigma}}{\sigma}\right) = \frac{RT'}{c_p}\left(\frac{dq}{dt} + \frac{\dot{\sigma}}{\sigma}\right) - \frac{1}{c_p} v_H . \nabla\Phi_s \tag{31}$$

where $\gamma = RT^*/ c_p$ and $c_p$ is the specific heat at constant pressure. The continuity equation becomes

$$\frac{dq'}{dt} + D + \frac{\partial \dot{\sigma}}{\partial \sigma} = \frac{1}{RT^*} v_H . \nabla \Phi_s \ . \tag{32}$$

Equations (31) and (32) have the same form as in Ritchie (1991) except that the inclusion of topography in the basic state solutions (28) and (29) has led to the explicit appearance of the Eulerian treatment (or kinematic) terms in the right-hand-sides of (31) and (32). The spatially-averaged and first-order off-centering treatments of these terms follow naturally from their presence in these right-hand-sides which are discretized as in Tanguay *et al.* (1992). The derivation and solution of the 3-dimensional Helmholtz equation proceeds as in Ritchie (1991) except that the unknown variables are P' and q' instead of P and q. Since

$$q' = \frac{P'(\sigma=1)}{RT^*}$$

$\Phi_s$ no longer appears directly in the vertical boundary conditions for this Helmholtz problem. In order to test the impact of the spatially-averaged Eulerian treatment of the mountains, tests were performed with a slightly modified version of this Canadian Global Spectral Forecast Model that is used for global data assimilation and medium-range forecasts at the Canadian Meteorological Centre (CMC). The version used in these tests had a triangular truncation with 119 waves and a timestep of 30 minutes. The modifications were to increase the timestep to 45 minutes (in order to provoke the resonance which is not present in the operational model), and to remove the physical parameterizations (so as not to obscure the response to this numerical problem). Figure 9 presents a 48 hour forecast of the 250 hPa geopotential height produced by this model with its semi-Lagrangian treatment of the mountains for the same case of strong flow across the Rockies as examined with the shallow water equations model in section 3 (figures 7 and 8). The unrealistic detail over Montana exhibits symptoms of the resonant behaviour and can be eliminated by reducing the timestep to the operational value of 30 minutes, or by removing the mountains. It can also be eliminated by changing to the spatially-averaged Eulerian treatment of the mountains, resulting in the forecast shown in figure 10. Note that the problem over Montana is removed without changing the forecast significantly elsewhere. No off-centering was used in this test. As in the nonlinear shallow water equations model, simply changing the mountain formulation without even using off-centering significantly reduces the fictitious numerical amplification of short scales in this baroclinic model.

For a more quantitative measure of the sensitivity to these two treatments of the mountains, the evolution of the northern hemisphere root-mean-square (rms) differences between forecasts produced with this simplified baroclinic model was examined in a series of integrations. First of all, the sensitivity to changing the mountain formulation was measured for integrations with a

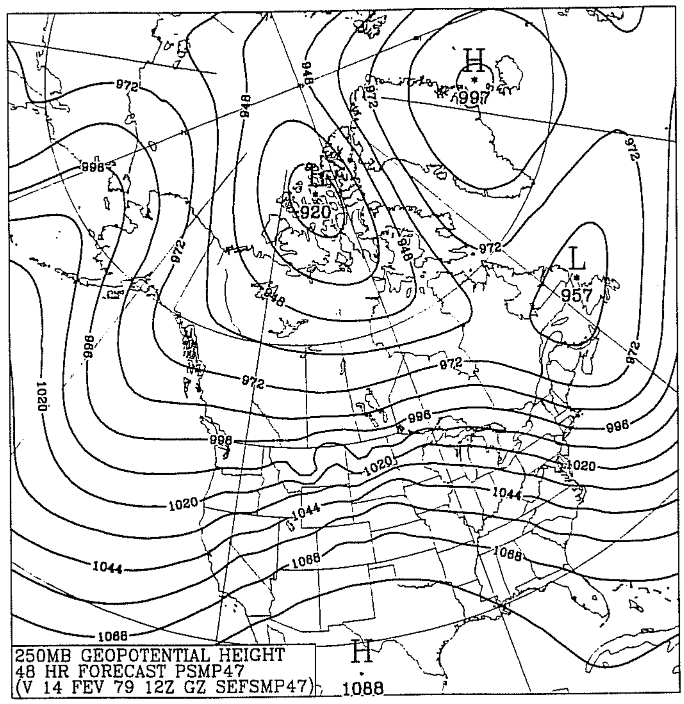


Fig.9 48 h forecast of the 250 mb geopotential height (dam), valid at 1200 UTC 14 February 1979, produced using a simplified baroclinic model with a semi-Lagrangian treatment of the mountains and a time step of 45 minutes. Contour interval 5 dam.

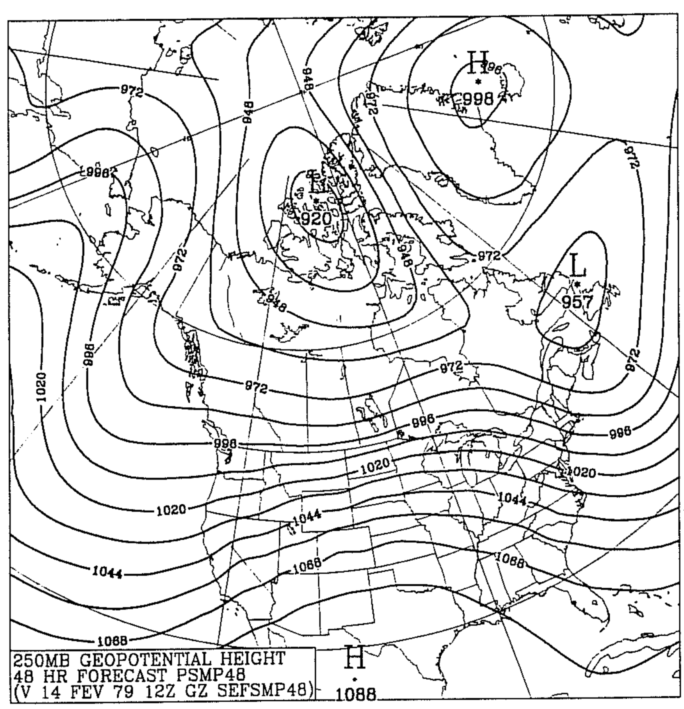


Fig. 10 As in Fig.9 except for a spatially-averaged Eulerian treatment of the mountains.

timestep that was short enough so that there would be no resonance problem and for which the time truncation errors would be small enough to permit these runs to be used as controls for the other tests. Figure 11 presents the evolution of the rms differences (in meters) between forecasts produced by the simplified baroclinic model with the semi-Lagrangian treatment of the mountains and the version with the spatially-averaged Eulerian treatment of the mountains, both using a 15 minute timestep. It is seen that the sensitivity to this change in mountain treatment is very small when the timestep is small. Figure 12 presents the sensitivity to changing the timestep in the version of the model using the spatially-averaged Eulerian treatment of the mountains. Here the timestep is trippled from 15 minutes as used in figure 11 to 45 minutes as used in figure 10. The sensitivity is at an acceptable level of less than 3 meters per day in the troposphere, establishing that the timestep used in figures 9 and 10 is not unreasonably large for this simplified model at this resolution. In particular, the 250 hPa geopotential height fields produced in the integrations with the 15 minute timestep (figure not shown) are visually very similar to figure 10 where the timestep is 45 minutes. Changing from the semi-Lagrangian treatment of mountains to the spatially-averaged Eulerian treatment appears in practice to significantly reduce the topographic resonance problem, permitting the use of larger timesteps that produce acceptable time truncation errors without provoking the fictitious numerical amplification of short scale waves.

## 5. DISCUSSION

In this paper we have compared two treatments of mountains in the context of three-time-level semi-implicit semi-Lagrangian models. Such models are susceptible to the spurious resonance that can develop in mountainous regions for Courant numbers larger than unity. Rivest *et al.* (1994) and Rivest and Staniforth (1995) recommended using a second-order instead of a first-order semi-implicit off-centering to suppress the spurious resonances, the former being more accurate. However, this requires the expense of additional time levels in the time integration scheme. The present study has showed that a first-order off-centering can be better suited when combined with a *spatially-averaged Eulerian* rather than a *semi-Lagrangian* treatment of mountains.

The simple linear one-dimensional analysis in section 2 showed that the resonance is much weaker with the spatially-averaged Eulerian treatment of mountains, and can be controlled with a much weaker first-order off-centering than with the semi-Lagrangian treatment of mountains that has been widely used in semi-Lagrangian models. In section 3 this was illustrated for the shallow water equations. The analytic and numerical linear solutions for the shallow water equations were reconstituted for the case of constant angular flow across an isolated "Gaussian hill". The presence of fictitiously amplified short waves was evident with both numerical treatments of the mountains, but these waves were much weaker with the spatially-averaged Eulerian treatment, and could be controlled with a much weaker off-centering than in the case with the semi-Lagrangian treatment of

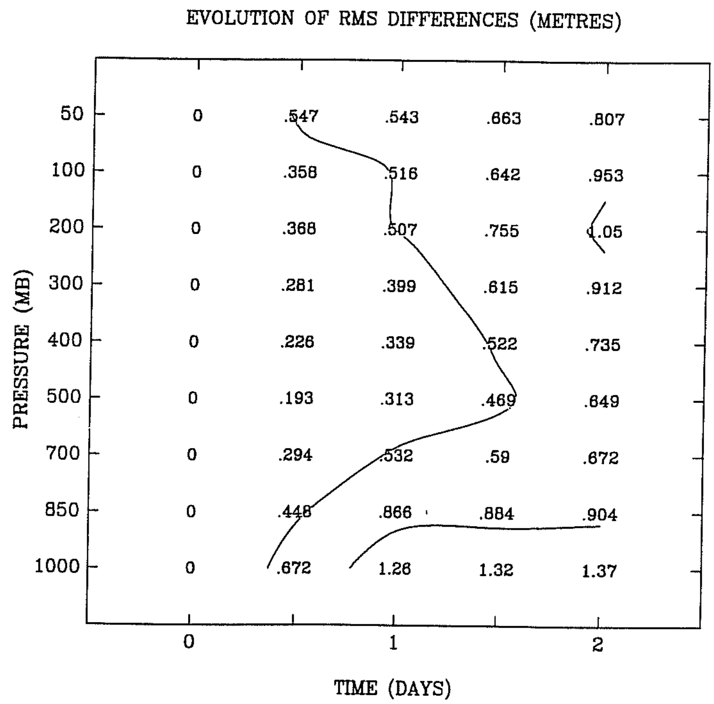


Fig.11 Evolution of the northern hemisphere rms differences (in meters) between forecasts produced by the simplified baroclinic model with the semi-Lagrangian treatment of the mountains and the version with a spatially-averaged Eulerian treatment of the mountains, both using a 15 minute time step. Contour interval 0.5 meter.

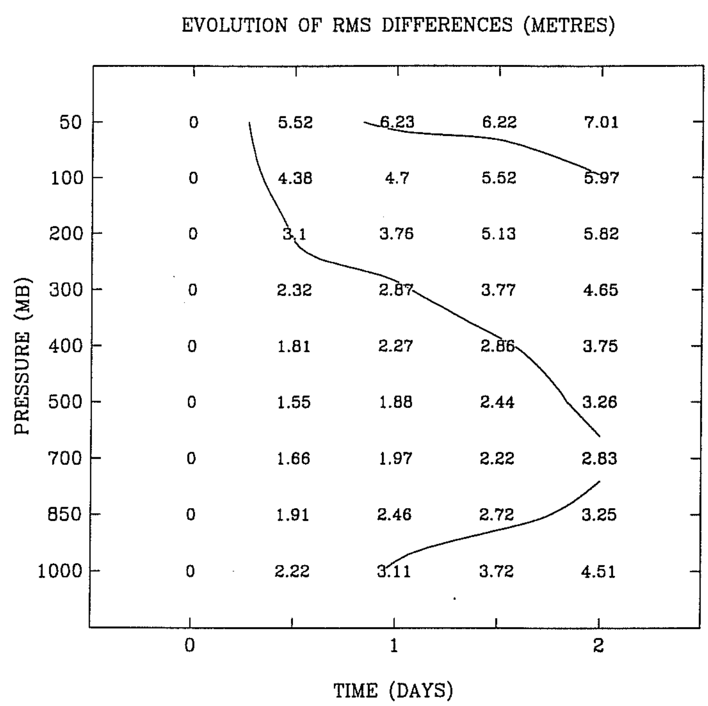


Fig.12 As in Fig.11 except comparing 15 minute and 45 minute time steps in the version of the model with a spatially-averaged Eulerian treatment of the mountains. Contour interval 3 meters.

the mountains. Tests with a nonlinear spectral shallow water equations model were also presented. For a real case of strong flow across the Rockies, short waves were evident over Montana and neighboring states in the version of the model using a semi-Lagrangian treatment of the mountains. The corresponding forecast using a version of the model with the spatially-averaged Eulerian treatment of the mountains showed that simply changing the mountain formulation without even introducing off-centering could significantly reduce the manifestation of numerical amplification.

A similar result was found in tests with a baroclinic model that were presented in section 4. By introducing topography in the basic state solution that is used for the semi-implicit treatment, the Eulerian treatment (or kinematic) terms emerge in the right-hand-sides of the perturbation thermodynamic and continuity equations. The spatially-averaged and first-order off-centering discretizations of these terms follow naturally in models that include these features for the other terms that are already present. Tests were performed with a simplified version of the Canadian Global Spectral Forecast Model for the same case of strong flow across the Rockies. Once again, unrealistic detail over Montana was eliminated simply by changing from the usual semi-Lagrangian to the spatially-averaged Eulerian treatment of the mountains, without using any off-centering. The local fictitious numerical amplification was controlled without changing the forecast significantly elsewhere.

The spatially-averaged Eulerian treatment of mountains appears to be a very effective, convenient, and inexpensive way of reducing the fictitious amplification of short scale waves due to topography in three-time-level semi-implicit semi-Lagrangian models. In particular, the code changes and extra computations are minimal for models that already have the spatial averaging feature. Although some off-centering or other damping mechanism is needed to formally eliminate the resonance, in practice with nonlinear models running from real data we have found that simply changing from the semi-Lagrangian to the spatially-averaged Eulerian treatment is sufficient to suppress the contamination of forecasts by unrealistic short scale details generated by the presence of topography. Consequently the time integration scheme retains its second-order accuracy. If some weak first-order off-centering eventually proves to be necessary, then there will be a correspondingly weak first-order time truncation error, but this combination would still represent an attractive alternative to a second-order off-centering needing extra time levels.

## 6. References

Bates, J.R., S. Moorthi and R.W. Higgins, 1993: A global multilevel atmospheric model using a vector semi-Lagrangian finite-difference scheme. Part I: Adiabatic formulation. *Mon. Wea. Rev.*, **121**, 244-263.

Coiffier, J., P. Chapelet, and N. Marie, 1987: Study of various quasi-Lagrangian techniques for numerical models. *Proceedings of ECMWF Workshop on Techniques for Horizontal*

*Discretization in Numerical Weather Prediction Models*, 19-46, European Centre for Medium-Range Weather Forecasts, Shinfield Park, Reading, U.K., 377 pp.

Côté, J., S. Gravel, and A. Staniforth, 1995: A generalized family of schemes that eliminate the spurious resonant response of semi-Lagrangian schemes to orographic forcing. *Mon. Wea. Rev.* , **123**, in press.

Héreil, P., and R. Laprise, 1995: Sensitivity of internal gravity wave solutions to the timestep of a semi-implicit semi-Lagrangian nonhydrostatic model. *Mon. Wea. Rev.*, **123**, submitted.

Kaas, E., 1987: The construction of and tests with a multi-level, semi-Lagrangian and semi-implicit limited area model. Diploma thesis, Geophysics Institute, Copenhagen University, Copenhagen, Denmark, 117 pp.

McDonald, A., and J.E. Haugen, 1992: A two time-level, three-dimensional semi-Lagrangian, semi-implicit, limited-area gridpoint model of the primitive equations. *Mon. Wea. Rev.*, **120**, 2603-2621.

Phillips, N.A., 1957: A coordinate system having some special advantages for numerical forecasting, *J. Meteor.*, **14**, 184-185.

Purser, R.J., and L.M. Leslie, 1994: An efficient semi-Lagrangian scheme using third-order semi-implicit time integration and forward trajectories. *Mon. Wea. Rev.*, **122**, 745-756.

Ritchie, H., 1988: Application of the semi-Lagrangian method to a spectral model of the shallow water equations. *Mon. Wea. Rev.*, **116**, 1587-1598.

Ritchie, H., 1991: Application of the semi-Lagrangian method to a multilevel spectral primitive-equations model. *Q.J.R. Meteorol. Soc.*, **117**, 91-106.

Ritchie, H., and C. Beaudoin, 1994: Approximations and sensitivity experiments with a baroclinic semi-Lagrangian spectral model. *Mon. Wea. Rev.*, **122**, 2391-2399.

Ritchie, H., C. Temperton, A. Simmons, M. Hortal, T. Davies, D. Dent, and M. Hamrud, 1995: Implementation of the semi-Lagrangian method in a high-resolution version of the ECMWF forecast model. *Mon. Wea. Rev.*, **123**, 489-514.

Rivest, C., A. Staniforth, and A. Robert, 1994: Spurious resonant response of semi-Lagrangian discretizations to orographic forcing: Diagnosis and solution. *Mon. Wea. Rev.*, **122**, 366-376.

Rivest, C., and A. Staniforth, 1995: Modifying the conventional three-time-level semi-implicit semi-Lagrangian scheme to eliminate orographically-induced spurious resonance. *Atmos. Ocean*, **33**, 109-119.

Robert, A., T.L. Yee and H. Ritchie, 1985: A semi-Lagrangian and semi-implicit numerical integration scheme for multilevel atmospheric models. *Mon. Wea. Rev.*, **113**, 388-394.

Tanguay, M., A. Simard and A. Staniforth, 1989: A three-dimensional semi-Lagrangian scheme for the Canadian regional finite-element forecast model. *Mon. Wea. Rev.*, **117**,1861-1871.

Tanguay, M., E. Yakimiw, H. Ritchie and A. Robert, 1992: Advantages of spatial averaging in semi-Lagrangian schemes. *Mon. Wea. Rev.*, **120**, 113-123.

Williamson, D.L., and J.G. Olson, 1994: Climate simulations with a semi-Lagrangian version of the NCAR CCM2. *Mon. Wea. Rev.*, **122**, 1594-1610.